Space time characterization II - Emission chronology

Roberta Ghetti* and Johan Helgesson*

*School of Technology and Society, Malmö University, SE-205 06 Malmö, Sweden

Abstract. Understanding the emission time sequence of neutrons, protons, and light charged particles can contribute to the understanding of the nuclear interaction and of the structure of nuclear matter, and it may even be sensitive to details of the nuclear equation of state, such as the density dependence of the nuclear symmetry energy. Small angle two-particle correlation functions can be used to deduce information on emission time distributions, and, in particular, on the emission chronology of different particle types. Furthermore, correlation functions from systems similar in size but with different isospin content (created in heavy ion collisions with isotope separated beam and/or target nuclei) are sensitive to the isospin dependence of the decay mechanism, and may be used as a probe for the density dependence of the nuclear symmetry energy.

Keywords: Heavy ion collisions, intensity interferometry, emission chronology, correlations, isospin
PACS: PACS numbers

SOURCES OF PARTICLE EMISSION

In a nucleus-nucleus collision at intermediate energy there are many sources of particle emission [1, 2, 3, 4, 5, 6]. To correctly interpret the experimental data, such as the extraction of emission time distributions, it is important to disentangle the contribution from the different sources.

In a central collision, fragments, nucleons and photons are initially emitted from first chance nucleon-nucleon collisions. These particles have a high energy and are emitted on a short time scale. After the initial first chance nucleon-nucleon collisions, a highly excited central source is formed. Initially, rather high energy nucleons and light fragments are emitted on a relatively short time scale. As the source equilibrates, the particles are emitted on a longer time scale with lower energy. Finally, nucleons are emitted on a long time scale over a large spatial region by secondary emission from excited fragments.

In semi-peripheral collisions, the initial emission of nucleons and fragments originates from first chance nucleon-nucleon collisions and is therefore similar to the scenario in a central collision. However, after the initial phase, the two nuclei pass through each other and emission first occurs from an overlap zone and later from neck-like region. This is accompanied by emission from the non-equilibrated residues. During these stages, high and intermediate energy particles are emitted on a relatively short time scale. The particles are emitted from spatially and velocity separated sources. Finally, nucleons will be emitted from equilibrated residues and by secondary emission from excited fragments. These nucleons are emitted on a long time scale over a large spatial region.

PARTICLE EMISSION TIME AND CHRONOLOGY

Particles originating from one specific source are emitted during a certain time interval. Normally, the rate of emitted particles changes during this time interval, leading to a specific time distribution for the source. If a two-particle correlation function of identical particles could be constructed from particles emitted from a single source (i.e. if the particle source could be isolated), and if the spatial distribution would be known, then the shape of the correlation function would yield information on the shape of the time distribution. Normally, neither the spatial nor the temporal distributions are known. In this case it is not straightforward to extract the spatial and time distributions from the shape of the correlation function. To interpret the experimental results, source models are often used. These source models contain some pre-assumption on the spatial and temporal distributions. The shape of these distributions can, to some extent, be varied by varying parameters of the model (such as radius and temporal width parameters). Such parameters then represent average emission point and average emission time, though it should be remembered that such average values are model dependent. In experimental data the situation is much more complex, since it is never possible to completely isolate one source from all the other sources present during the reaction. The contribution from several

sources leads to a total time distribution with a complex shape, where the effective average emission time will depend on different factors.

What one is usually referring to with *emission chronology* is a difference in the average emission times between two particle types. Though, it is worth noticing that the emission times of the two particles may overlap to a large extent, and the difference in their respective average emission times can be small compared with the width of the emission time distributions. Furthermore, if different sources contribute, like in peripheral reactions, they contribute to a complex time distribution of the emitted particles. As an example, we can consider two particle types emitted from two sources. Different origins for different average emission times can be recognized: One origin could be a simple shift of two similar time distributions. Another origin could be that the width of the time distributions are different, while their shape is quite similar. Finally, it is also possible to think that, if more than one source is contributing, the relative weight of the sources is different for the two particle types, leading to different average emission times. In a real reaction all of the above reasons contribute, with a different weight depending for example on applied gates, selected angular ranges, etc.

Even though the extraction of the emission times and sequences is quite involved, there is a wealth of experimental information that is available. A great advantage is to perform simultaneous measurements of both like and unlike particle correlation functions. By applying different gates, such as polar angle gates, total momentum gates, directional gates, velocity gates for unlike particles, etc., certain sources are enhanced relative to others. For instance, non-equilibrium emission can be enhanced by high and intermediate total momentum gates, while particles from evaporation and excited fragments can be suppressed by shape analysis discarding the very low relative momentum region. Furthermore, single particle information, such as energy spectra at different angles, should be used in the analyses. A systematic study can therefore to a large extent disentangle the space-time characteristics of the contributing sources, by putting strong constraints on theoretical models [7].

Emission chronology from like particle correlations

The emission chronology between two particle types can, under certain conditions, be determined from like-particle correlation functions. If it is valid to assume that both particle types are emitted from the same spatial region, a fit with a calculated correlation function, based on some source function, to the experimental correlation function, will yield an average emission time for each particle type. By comparing these average emission times, an emission chronology can be inferred. For a review, see Ref. [8] and references therein. The same method can also be used to determine differences in emission times for the same particle type emitted from different systems but with the same spatial region, for instance, different neutron emission times from systems similar in size and energy content, but with different isospin content (see next section).

The drawback of this method is that the results are sensitive to the assumption of emission from the same spatial region. Furthermore, the extracted average emission times are model dependent, since the average emission times depend on the pre-assumption of the shape of the (spatial and) temporal distributions assumed by the specific source model.

Emission chronology from unlike particle correlations

Model independent information on the emission chronology of two particle types can instead be obtained from unlike-particle correlation functions. If there is a difference in the average emission times, it is possible, by suitable gates, to divide the particle pairs into two classes with different average distances when the two particles "start to interact". Since the strength of the final state interaction depends on the distance between the particles, this will lead to a different strength of the correlation function for the two classes. By comparing these correlation functions, the emission chronology can then be inferred without any model assumptions.

Below we present the details of this technique. An important assumption for this method to be valid is that the particles are emitted independently. Furthermore, certain assumptions (which depends on the used gates) must be made on the spatial region from which the particles are emitted.

Velocity gated correlation functions

A technique to probe the emission sequence and time delay of ejectiles in nuclear reactions was first suggested for charged particle pairs, based on the idea that mutual Coulomb repulsion would be experienced by pairs of charged particles emitted with a short time delay. Comparison of the velocity difference spectra with trajectory calculations would thus give a measure of the average particle emission sequence [9, 10, 11].

The technique was extended to any kind of interacting, non-identical particle pairs in the theoretical study of Ref. [12]. There it was demonstrated that the sensitivity of the correlation function to the asymmetry of the distribution of the relative space-time coordinates of the particle emission points can be used to determine the differences in the mean emission times by applying energy or velocity gates. This effect has been proposed for particle pairs such as pd and np [12], $p\pi$ [13], K^+K^- [14].

Velocity gated correlation functions of non-identical particles is a very powerful tool to investigate emission sequences in nuclear collisions [15]. The basic idea is that, if there is an average time difference in the emission times of two particles types, there will also be a difference in the average distance for particle pairs selected with the condition $v_1 > v_2$ as compared to the pairs selected with the complementary condition $v_1 < v_2$. This is because the particle emitted first will, on average, travel a different distance in the two complementary classes (due to the different velocities) before the second particle is emitted. In particular, the interaction is enhanced for those pairs for which the average distance is smaller. This can be easily seen if one compares the correlation function $C_1(q)$, gated on pairs $v_1 > v_2$, with the correlation function $C_2(q)$, gated on pairs $v_1 < v_2$. If particle 2 is emitted earlier (later) than particle 1, than the condition $v_1 > v_2$ will sample smaller distances (larger correlations) than the complementary condition $v_1 < v_2$. Therefore the ratio C_1/C_2 will show a peak (dip) in the region of relative momentum q where there is a correlation and a dip (peak) where there is an anti-correlation. Furthermore the ratio C_1/C_2 will approach unity both for $q \to 0$ (since the velocity difference of the two emitted particles is negligible) and $q \to \infty$ (since modifications of the two-particle phase space density arising from final state interactions are negligible). The exact location of the peak and dip in the ratio depends on the source, and in particular on the origin of the difference in the average emission times.

Experimental results

At low energies, the analysis of two-particle correlations and velocity difference spectra has allowed to find results consistent with the statistical compound nucleus decay for the light products emitted from the reactions ^{16}O + ^{10}B (E_{lab} = 62.5 MeV), and ^{16}O + ^{12}C (64.0 MeV). The method could also be used for the determination of fission time scales [16].

At intermediate energies, the time sequence of p and d has been deduced for the $E/A = 50$ MeV Xe + Sn reaction studied by the INDRA collaboration. An average emission of deuterons $\approx$ 250 fm/c earlier than protons has been explained as the result of averaging over a long time sequence between pre-equilibrium and thermal emission for protons, whereas deuteron emission, resulting mainly from hard nucleon-nucleon collisions, is concentrated at a few tens of fm/c [17].

First experimental evidence of the emission chronology of neutrons and protons deduced from the np correlation function, was reported in Ref. [15] for the $E/A = 45$ MeV ^{58}Ni+ ^{27}Al reaction measured by the CHIC collaboration at LNS, Catania. The experimental results from differently gated correlation functions were in qualitative agreement with the Koonin-Pratt formalism [18, 19]. It was claimed that for high-parallel-velocity and high-total-momentum selected events that enhance projectile residue and/or intermediate velocity sources, the proton is, on average, emitted earlier than the neutron.

In Ref. [20] the emission time chronology of neutrons, protons, and deuterons, was presented for the $E/A = 61$ MeV ^{36}Ar + ^{27}Al reaction measured at KVI, Groningen. The experimental results showed that the angular and total-momentum dependences of the pp and np correlation functions support a dissipative binary reaction scenario, where early dynamical emission is followed by statistical evaporation. The reverse kinematics utilized in the experiment, and fairly high energy thresholds, enhanced the early dynamical emission component in the backward measurement. The analysis of velocity-gated correlations of non-identical particle pairs yielded detailed information about the particle emission time sequence. The results from the np "backward" measurement are shown in Fig. 1, right column (from Ref. [20]). The dip in the C_n/C_p ratio indicates that neutrons are, on the average, emitted earlier than protons. For the "forward" measurement (Fig. 1, left column), the shape of the correlation function exhibits a correlation at q<40 MeV/c and a small anti-correlation at 40 <q< 100 MeV/c, and the pairs with v_n>v_p contributing to C_n interact more

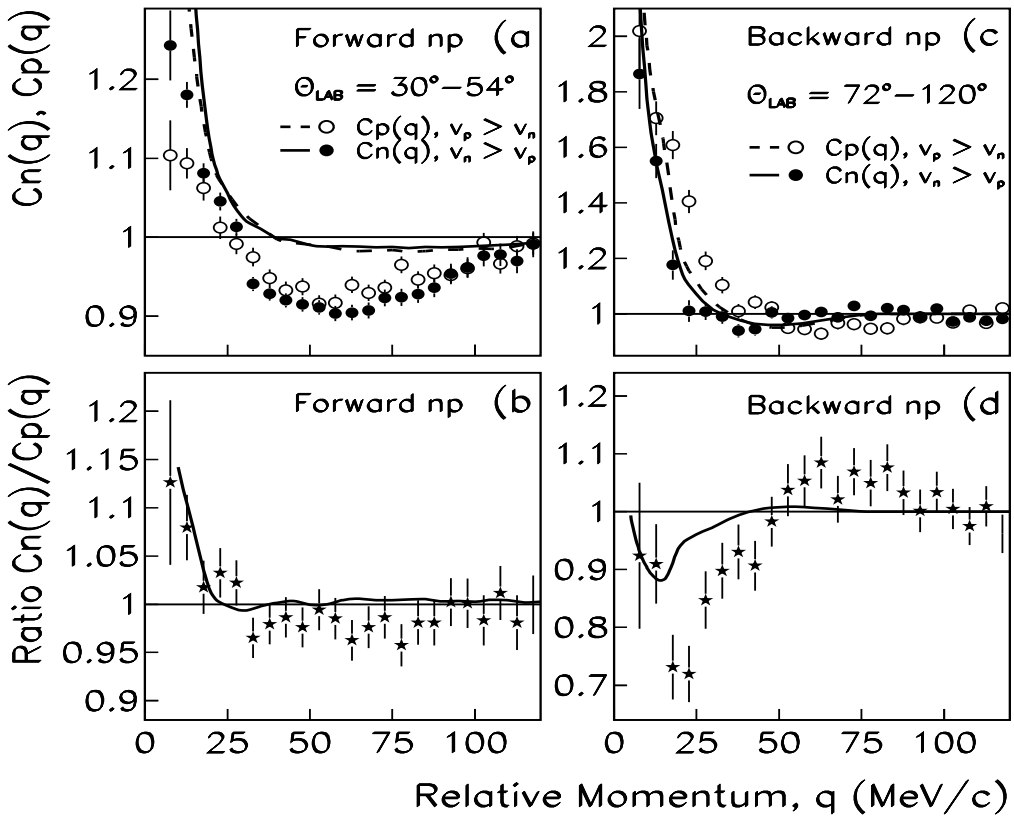

FIGURE 1. From the $E/A = 61$ MeV ^{36}Ar + Al reaction measured at KVI, velocity-gated *np* correlation functions (C_n, filled circles, and C_p, open circles) and their ratio (C_n/C_p) Left column: forward measurement. Right column: backward measurement. The lines are results from model calculations. From Ref. [20].

strongly. This indicates that protons are, on the average, emitted earlier than neutrons, a result in agreement with that obtained for the $\theta_{lab} \approx 45^o$ E/A = 45 MeV ^{58}Ni + Al reaction [15]. The complete sequence of average emission times, τ, extracted from the $E/A = 61$ MeV ^{36}Ar + Al reaction was: For the dynamical emission source, $\tau_n < \tau_d < \tau_p$; for the projectile residue emission, $\tau_d < \tau_p < \tau_n$. The interpretation of these results, presented in Ref. [20], highlights the importance of the contribution from the different emission sources.

The technique of Ref. [12] has also been applied to pairs of non-identical light charged particles produced in central collisions of heavy ions in the A = 100 mass region at a beam energy of 400 MeV/nucleon, measured with the FOPI detector system at GSI [21]. The difference between longitudinal correlation functions with the relative velocity parallel and anti-parallel to the center-of-mass velocity of the pair in the central source has allowed the extraction of apparent space-time differences of the emission of the charged particles. Comparing the correlations with results of a final-state interaction model, delivered quantitative estimates of these asymmetries. Time delays as short as 1 fm/c or - alternatively - source radius differences of a few tenth fm were resolved. The strong collective expansion of the participant zone introduces not only an apparent reduction of the source radius but also a modification of the emission times. After correcting for both effects a complete sequence of the space-time emission of $p, d, t, {}^3He, K$ particles was extracted.

At even higher energy regimes, the above method has been used to tackle the problem of the possible observation of strangelets in the frame of the distillation process following the creation of a quark gluon plasma. In this case, strange and anti-strange particles may not be produced at the same time in a baryon rich system under low bag constant scenarios. Such a prediction has been tested using K^+K^- correlations in Ref. [22].

ISOSPIN EFFECTS AND PERSPECTIVES FOR THE ASY-EOS

The isospin dependence of the nuclear equation of state is probably the most uncertain property of neutron-rich matter. This property is essential for the understanding of extremely asymmetric nuclei and nuclear matter as it may occur in the *r*-process of nucleosynthesis or in neutron stars. In order to study the isospin-dependent EOS, heavy ion collisions with isotope separated beam and/or target nuclei can be utilized. In these collisions, excited systems are created with varying degree of proton-neutron asymmetry and a noticeable isospin dependence of the decay mechanism is expected [23]. By selecting semi-peripheral collisions, the symmetry term of the EOS is probed at low densities, while central collisions are expected to be sensitive to the high density dependence.

Theoretical predictions

Recently, the two-nucleon correlation function has been considered as a probe for the density dependence of the nuclear symmetry energy [24, 25, 26]. In these theoretical studies with an isospin-dependent IBUU transport model, it was shown that the density dependence of the symmetry term of the EOS affects the temporal and spatial structure of reaction dynamics by affecting the average emission times of neutrons and protons as well as their relative emission sequence. For central collisions, a stiff EOS causes high momentum neutrons and protons to be emitted almost simultaneously, thereby leading to strong correlations. A soft EOS delays proton emission, which weakens the *np* correlation [24, 25]. It was found that the symmetry energy effect becomes weaker with increasing impact parameter and incident energy. Also, the strength of nucleon-nucleon correlation function is reduced in collisions of heavier reaction systems as a result of larger nucleon emission source [25]. It was further found that the momentum dependence of both isoscalar nuclear potential and the symmetry potential influences significantly the space-time properties of the nucleon emission source. Specifically, the momentum dependence of the nuclear potential reduces the sensitivity of two-nucleon correlation functions to the stiffness of the nuclear symmetry energy [26].

In spite of the large uncertainties in the symmetry potential, and in particular in the momentum dependent part, the exploratory studies in [24, 25, 26] are very encouraging for using two-particle correlations to study the symmetry potential. It is also important to remember that the symmetry interaction does not only influence the dynamical emission of particles from the overlap and neck-like regions, but also the formation of the residues. Therefore also the particles emitted from the residues contain information on the symmetry energy. To make improvements in the future on the understanding of the symmetry potential, it is needed to have models that consistently can describe both the dynamical emission of particles and the formation of residues and their subsequent pre-equilibrium and equilibrium emission of particles. By applying the experimental conditions and systematically comparing calculated and experimental energy spectra and gated correlation functions for like and unlike particles, it will be possible to obtain hard constraints on the symmetry potential.

Experimental results

First experimental results have been obtained on two-particle correlation functions from systems similar in size, but with different isospin content [27]. Small-angle two-particle correlation functions with neutrons and protons have been obtained from semi-peripheral E/A = 61 MeV Ar + ^{112,124}Sn collisions measured at the AGOR cyclotron of KVI. The interferometer consisted of 16 CsI(Tl) crystals for light charged particles detection (θ_{lab}=30°–114°) and 32 liquid scintillators for neutron detection (θ_{lab}=36°–120°).

Emission from the different sources was enhanced/suppressed by introducing angular cuts (intermediate velocity source emission is enhanced forward, target residue emission is enhanced backwards) and cuts in the total momentum (P_{tot}) of the particle pair, calculated in the relevant emission source frame. Fig. 2 (from Ref. [28]) presents the *pp* correlation function for particle pairs selected within the three different gates.

1. Particles emitted by the intermediate velocity source at prompt dynamical emission stage, (e.g. first-chance nucleon-nucleon collisions), are enhanced by selecting high-P_{tot} pairs in the intermediate velocity source frame. For the sample of *pp* pairs, the angular range $30^o \leq \theta \leq 42^o$ is used for this gate.
2. Particles emitted by the intermediate velocity source at later dynamical emission stage (e.g. neck-emission), are enhanced by selecting intermediate-P_{tot} pairs in the intermediate velocity source frame. Again, the angular range $30^o \leq \theta \leq 42^o$ is utilized for *pp* pairs.

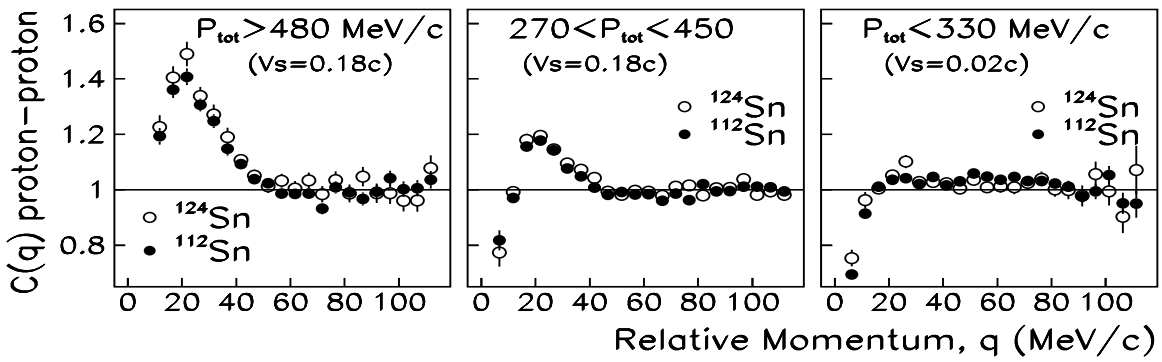

FIGURE 2. For ^{36}Ar + ^{112}Sn (filled circles) and ^{36}Ar + ^{124}Sn (open circles) collisions, *pp* correlation functions. Left: *pp*, high-P_{tot}, $30^o \leq \theta \leq 42^o$. Middle: *pp*, intermediate-P_{tot}, $30^o \leq \theta \leq 42^o$. Right: *pp*, low-$P_{tot}$, $54^o \leq \theta \leq 114^o$. From Ref. [28].

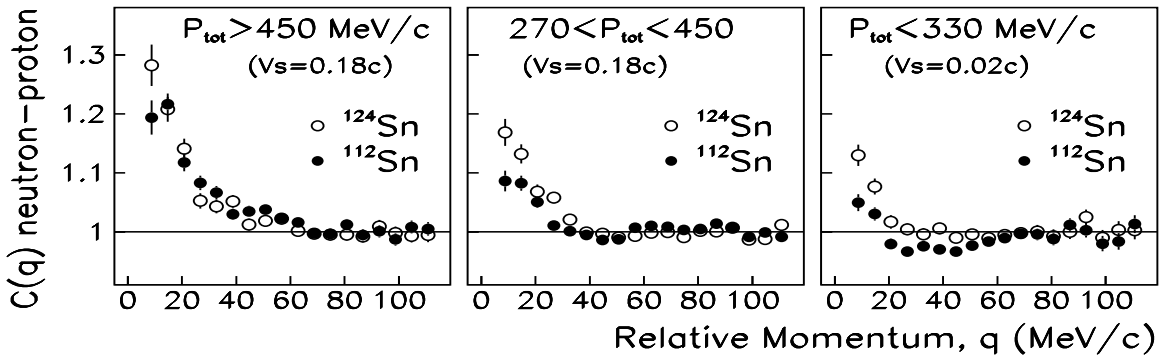

FIGURE 3. For ^{36}Ar + ^{112}Sn (filled circles) and ^{36}Ar + ^{124}Sn (open circles) collisions, *np* correlation functions. Left: *np*, high-P_{tot}, $30^o \leq \theta \leq 120^o$. Middle: *np*, intermediate-P_{tot}, $30^o \leq \theta \leq 120^o$. Right: *np*, low-$P_{tot}$, $54^o \leq \theta \leq 120^o$. From Ref. [28].

3. Particles emitted by the target residue are enhanced by selecting low-P_{tot} pairs in the target residue frame. The angular range $54^o \leq \theta \leq 120^o$ is applied to both *pp* and *np* pairs. The neutron energy threshold is set to 8 MeV for this gate.

One can notice that the height of the peak at $q \sim 20$ MeV/c is progressively reduced going from gate 1 to gate 3, indicating an increase in the particle emission time. Fig. 3 presents the corresponding results for the *np* correlation function. By comparing the results for the two Sn targets, one can see an isospin effect, particularly in gate 1 for *pp* and in gates 2 and 3 for *np*, where the height of the correlation function is larger for the more neutron-rich target. This indicates a shorter average emission time for this system.

For the interpretation of the correlation data, it is important to note that the correlation function depends on the space-time extent of the emitting source. From the size of the source, a stronger correlation is expected for the smaller ^{36}Ar + ^{112}Sn system, an effect expected also because of the larger excitation energy per particle available for this system (yielding a shorter emission time). On the other hand, the change in neutron number implies a different symmetry energy which also affects the *n* (and *p*) emission times. Neutrons are expected to be emitted faster in the neutron-rich system, which would lead to an enhancement of the correlation strength for ^{36}Ar + ^{124}Sn. Thus, the net influence on the correlation function is not easily predictable, both due to the uncertainty in the symmetry energy and to the presence of more than one source of emission. The stronger *np* correlation observed for the larger Ar + ^{124}Sn system in the low-total-momentum gate may indicate that the more asymmetric system generates a more asymmetric and excited target residue, that, consequently, decays on a faster time scale.

More insight into these results has been gained by performing an analysis of the particle emission time sequence in Ref. [29]. In all studied angle and total-momentum gates, it was found that neutrons are, on average, emitted earlier than protons. Furthermore, the shorter *np* emission time scale for the Ar + ^{124}Sn system results from a faster emission of the neutrons, as compared to the Ar + ^{112}Sn system. This is particularly true for the particles emitted from the target

residue, indicating that the residues in the two reactions were formed differently due to the symmetry interaction. Further experimental results of particle emission sequence involving deuterons indicate that for the Ar + ^{124}Sn system neutrons are emitted slightly earlier than deuterons, again a result pointing to a faster neutron emission for the more neutron rich system. Deuterons, being formed mainly by coalescence, appear to have emission time that falls in-between that of neutrons and protons. No sizeable isospin effects in the emission sequence of deuterons and protons were found for the above mentioned systems.

While the above mentioned results are at the moment the only existing experimental results on the isospin dependence of the two-particle pp and np correlation functions, a more focused investigation is going to be undertaken in a new series of interferometry experiments. At the Superconducting Cyclotron of LNS, Catania, pp, nn and np correlations will be measured in the later half of 2005 for the reactions ^{112,124}Sn + ^{58,64}Ni and ^{112,124}Sn + ^{112,124}Sn at beam energy of 35 MeV/nucleon.

REFERENCES

1. C.P. Montoya, *et al.*, Phys. Rev. Lett. **73**, 3070 (1994).
2. Y. Larochelle *et al.*, Phys. Rev. C **59**, R565 (1999).
3. E. Plagnol *et al.*, Phys. Rev. C **61**, 014606 (1999).
4. J. Łukasik *et al.*, Phys. Lett. B, **566**, 76 (2003).
5. T. Lefort *et al.*, Nucl. Phys. **A 662**, 397 (2000).
6. Ph. Eudes, Z. Basrak and F. Se'bille, Phys. Rev. C **56**, 2003 (1997).
7. G. Verde *et al.*, WCI white paper, Space-Time Characterization, I.
8. D. Ardouin, Int. J. Mod. Phys. E**6**, 391 (1997).
9. C. J. Gelderloos and J. M. Alexander, Nucl. Instrum. Methods A **349**, 618 (1994).
10. C. J. Gelderloos et al., Phys. Rev. Lett. **75**, 3082 (1995);
11. C. J. Gelderloos et al., Phys. Rev. C **52**, R2834 (1995).
12. R. Lednicky, V.L. Lyuboshitz, B. Erazmus, D. Nouais, Phys. Lett. B **373**, 30 (1996).
13. S. Voloshin, R. Lednicky, S. Panitkin, and N. Xu, Phys. Rev. Lett. **79**, 4766 (1997).
14. D. Ardouin et al., Phys. Lett. B **446**, 191 (1999).
15. R. Ghetti, *et al.*, Phys. Rev. Lett. **87**, 102701 (2001).
16. M.M. de Moura *et al.*, Nucl. Phys. **A 696**, 64 (2001).
17. D. Gourio *et al.*, Eur. Phys. J. **A 7**, 245 (2000).
18. S.E. Koonin, Phys. Lett. B **70**, 43 (1977).
19. S. Pratt and M.B. Tsang, Phys. Rev. C **36**, 2390 (1987).
20. R. Ghetti, *et al.*, Phys. Rev. Lett. **91**, 092701 (2003).
21. R. Kotte, *et al.*, Eur. Phys. J. A**6**, 185 (1999).
22. S. Soff *et al.*, Journ. Phys. **G23**, 789 (1997).
23. B.A. Li, *et al.*, WCI white paper, III-Isospin properties.
24. L.W. Chen, V. Greco, C.M. Ko, Bao-An Li, Phys. Rev. Lett. **90**, 162701 (2003).
25. L. W. Chen, V. Greco, C.M. Ko, Bao-An Li, Phys. Rev. C **68**, 014605 (2003).
26. L. W. Chen, C.M. Ko, Bao-An Li, Phys. Rev. C **69**, 054606 (2004).
27. R. Ghetti *et al.*, Phys. Rev. C **69**, 03160 (2004).
28. R. Ghetti and J. Helgesson, Nucl. Phys. **A 752**, 480c (2005).
29. R. Ghetti *et al.*, Phys. Rev. C **70**, 034601 (2004).